Cell PRESS
Chemistry & Biology
Article

A Metabolomic View of *Staphylococcus aureus* and Its Ser/Thr Kinase and Phosphatase Deletion Mutants: Involvement in Cell Wall Biosynthesis

Manuel Liebeke,[1] Hanna Meyer,[1,3] Stefanie Donat,[2,3] Knut Ohlsen,[2] and Michael Lalk[1,*]
[1]Institute of Pharmacy, University of Greifswald, F.-L.-Jahn Strasse 17, 17487 Greifswald, Germany
[2]Institute of Molecular Infection Biology, University of Würzburg, J.-Schneider Strasse 2/Bau D15, 97080 Würzburg, Germany
[3]These authors contributed equally to this work
*Correspondence: lalk@uni-greifswald.de
DOI 10.1016/j.chembiol.2010.06.012

SUMMARY

Little is known about intracellular metabolite pools in pathogens such as *Staphylococcus aureus*. We have studied a particular metabolome by means of the presented LC-MS method. By investigating the central carbon metabolism which includes most of the energy transfer molecules like nucleotides, sugar mono- and biphosphates, and cofactors, a conclusion about phenotypes and stress answers in microorganisms is possible. Quantitative metabolite levels of *S. aureus* grown in complex lysogeny broth and in minimal medium were compared in the wild-type *S. aureus* strain 8325 and the isogenic eukaryotic-like protein serine/threonine kinase (Δ*pknB*) and phosphatase (Δ*stp*) deletion mutants. Detection of several remarkable differences, e.g., in nucleotide metabolism and especially cell wall precursor metabolites, indicates a previously unreported importance of serine/threonine kinase/phosphatase on peptidoglycan and wall teichoic acid biosynthesis. These findings may lead to new insights into the regulation of staphylococcal cell wall metabolism.

INTRODUCTION

There is an urgent need for new antimicrobial drugs, especially against *Staphylococcus aureus* and its methicillin-resistant strains (Payne, 2008). These Gram-positive bacteria have their natural habitat on human skin and mucosa, acting as opportunistic pathogens, and causing a broad range of nosocomial and community acquired infections (Lowy, 1998). A challenge in treating *S. aureus* infections is increasing drug resistance. These so-called ''superbugs'' have acquired resistance to multiple drugs from penicillin/methicillin to quinolone and also vancomycin (Nordmann et al., 2007). Rapid adaption to stress conditions such as antibiotic treatment and the environmental changes experienced upon entry into the human habitat, e.g., nutrient limitation or anaerobic conditions, makes *S. aureus* an important subject of research (Hecker et al., 2009). Discovery of new antibiotic targets such as the connections between virulence and metabolism of *S. aureus* requires improved understanding of its physiology (Somerville and Proctor, 2009). It is therefore of central importance to decipher its metabolome. In the postgenomic era, despite the large sets of genomic, transcriptomic, and proteomic data available for *S. aureus* (Becker et al., 2007), there is lack of comprehensive qualitative and quantitative metabolomic data (Fiehn et al., 2000). Computer calculations of metabolic pathways (in silico modeling) for *S. aureus* based on published data, genome-scale reconstruction, annotations, and use of other databases yielded 571 and 712 physiological metabolites involved in *S. aureus* strain N315 metabolism (Becker and Palsson, 2005; Heinemann et al., 2005).

Uncovering the unique metabolome of a cell requires a series of analytical techniques, the so-called metabolic platform (van der Werf et al., 2007). The most commonly used separation methods in metabolomics research are liquid chromatography (LC) and gas chromatography (GC) coupled with mass spectrometric (MS) detection. A comprehensive review of these methods has been presented (Villas-Boas et al., 2005). The most significant marker substances for the physiological status of the cell are the polar compounds, including uridine, guanosine, cytosine, and adenosine phosphates and glycolysis intermediates, as well as cofactors and redox balance substances. Glucose-6-phosphate and its upstream metabolites are important physiological indicators under conditions of nutrient deprivation, as well as highly phosphorylated guanosine nucleotides such as the stringent response messenger (p)ppGpp) (Crosse et al., 2000). Cofactors like NAD^+/H, $NADP^+$/H, FMN, FAD^+/H, CoA, Acetyl-CoA, and others provide information on the redox status of the cell (Richardson et al., 2008). Adenosine phosphates are essential to inform about energy charge changes.

Detecting and quantifying metabolites with rapid turnover under conditions of adaptation to stress such as antibiotic treatment or environmental influences are important to reveal aspects of the relevant physiology. A major drawback of prominent GC/MS-based metabolome analysis methods is the high detection limit of the above-mentioned substances. This is due largely to their instability under the necessary temperature-dependent derivatization procedures for volatilization. We have, therefore, developed an extensive reliable LC/MS method to analyze all of the above mentioned metabolites in *S. aureus* in one run. CE/MS (Feng et al., 2008) or HPLC/MS with HILIC columns (Bajad et al., 2006) as well as standard RP-C18 columns with ion pairing reagents for polar metabolites detection and

quantification has recently been shown to allow more accurate quantitation of a wider range of compounds (Cordell et al., 2008; Coulier et al., 2006; Lazzarino et al., 2003). Further development of these methods enabled us to analyze other important compound groups such as cofactors and cell wall precursors. This method also analyzes unknown polar compounds, further enhancing our understanding of the metabolome (Kind et al., 2009).

The analytical method introduced above was used to study the metabolome of *S. aureus* 8325 in two different growth media (complex and chemical defined). A metabolome comparison of the wild-type and its phosphatase/kinase deletion mutants Δ*pknB* and Δ*stp* was performed in detail.

Reversible phosphorylation or dephosphorylation of proteins plays an important role in a variety of cell processes (Beltramini et al., 2009). Regulation of cell differentiation, signal transduction, and metabolism is dependent on specific phosphorylation states of the cognate regulatory proteins. Signal transduction, dependent on phosphorylation of specific histidine, aspartate, serine and threonine, and tyrosine residues of proteins, is known in eukaryotes and bacteria (Deutscher et al., 2006). Different serine/threonine and tyrosine phosphorylated proteins have been identified in *S. aureus*. They belong among others to central carbon metabolism (enolase, triose isomerase, fructose biphosphate aldolase, pyruvate dehydrogenase, phosphate acetyl transferase, and glyoxalase family protein [SA 1340]), as well as the protein synthesis pathway (Lomas-Lopez et al., 2007). PknB is a eukaryotic-like serine/threonine kinase (ESTK or STK), whereas the function of STP (named YloO in *Bacillus subtilis*) is a serine/threonine phosphatase (ESTP or STP) (Beltramini et al., 2009; Ohlsen and Donat, 2009). A recent transcriptome study of *S. aureus* 8325 and its isogenic Δ*pknB* mutant revealed a major influence of PknB on expression profiles of purine and pyrimidine biosynthesis, cell wall metabolism, autolysis, and glutamine synthesis genes under normal growth conditions in complex LB medium (Donat et al., 2009). It was also shown that deletion of *pknB* increased the susceptibility to cell wall-active antibiotics such as methicillin and tunicamycin, as well as Triton X-100 induced lysis, whereas the phosphatase deletion mutant behaved as the wild-type (Beltramini et al., 2009; Donat et al., 2009). In accordance with the thicker cell wall of the STP mutant, lysostaphin, a peptidoglycan-targeting glycineglycine endopeptidase, showed decreased ability to lyse cells (Beltramini et al., 2009). Infection related studies of both the *pknB* and *stp* mutants showed a clear link to virulence in a mouse model for the kinase mutant, predicting a crucial role in *S. aureus* pathogenesis (Debarbouille et al., 2009). Further investigation of these *S. aureus* mutant strains is required in order to better understand their physiology.

Here, we report findings derived using an analytical IP-LC/MS method that gathers reproducible metabolite data from intracellular samples. The results obtained for *S. aureus* 8325 constitute quantitative measurements of a majority of central pathway metabolites in staphylococci. In addition, the results for the kinase mutant are congruent with the recently described transcriptome data and phenotypic observations (Beltramini et al., 2009; Debarbouille et al., 2009; Donat et al., 2009). A regulatory interplay between the serine/threonine kinase/phosphatase system and cell wall metabolism in *S. aureus* is clearly demonstrated. This study facilitates the next step toward a system biological approach of this versatile pathogen *S. aureus*, and the LC/MS method described herein is suitable for studies with other microbial metabolomes.

RESULTS

Analysis of *S. aureus* Metabolome

The metabolite profiles of *S. aureus* 8325 grown in chemical defined medium (CDM) to exponential phase (OD_{500} = 1) or complex medium to exponential, mid-exponential, and late exponential growth phase OD_{540} = 1, 2, and 3) (Figure 1) were investigated by IP-LC/MS. We were able to identify 79 metabolites in *S. aureus* samples cultured in both chemically defined medium (CDM) and lysogeny broth (LB). Absolute quantification relative to cell dry weight (CDW) (Meyer et al., 2010) was performed for 21 of these. The remaining compounds were quantified relative to CDW by their parent ion intensity $[M\text{-}H]^-$.

By using this new method, all metabolites reported in Table 1 could be detected in a single LC/MS run within 65 min. With an automated MZmine peak detection (Katajamaa et al., 2006), a more complex list of mass traces could be evaluated from the *S. aureus* samples. Nevertheless, only compounds with a reference substance analyzed by our method were considered for metabolome interpretations (for identification and quantification details, see Figures S2 and S3 available online).

For evaluation of the extraction and analytical protocol, the adenylate energy charge (AEC = [(ATP) + 0.5 * (ADP)] / [(ATP) + (ADP) + (AMP)] of the cells was determined. This ratio considers concentrations of AMP, ADP, and ATP, i.e., metabolites with the highest turnover in cells (e.g., $t_{half\text{-}life}$(ATP) < 0.1 s). The AEC is one prominent benchmark to help characterize the physiological status of sampled organisms (Atkinson, 1968), especially to compare data with previously documented metabolomics studies (Ewald et al., 2009; van der Werf et al., 2008). An experimental AEC between >0.8 and <1.0 for exponential phase, nutrient unlimited cells indicates a successful quenching/sampling and extraction protocol. Nevertheless, a positive AEC reflects only stable adenylates but does not exclude other biochemical side reactions. The AEC obtained for both the wild-type and mutants were highly reproducible (see Table 2). AEC for LB-grown cells were calculated to be between 0.75 and 0.88 and for CDM the AEC was between 0.88 and 0.92. With increasing cultivation time and concomitant higher cell densities in complex medium, the cells may be nutrient limited and the AEC dropped slightly until the stationary growth phase was reached (see insets in Figure 1), in agreement with the literature (Hutchison and Hanson, 1974; Tynecka et al., 1999).

Overall quantitative nucleotide levels are of keen interest for metabolic network calculations. For example, when done on a genome scale, Heinemann et al. (2005) assumed ATP consumption rates based on literature data from other microorganisms. We measured nucleotide levels for exponentially phase LB-grown cells of ~12 $\mu mol/g_{CDW}$ ATP (for comparison: *Escherichia coli,* 7 $\mu mol/g_{CDW}$ [Meyer et al., 1999]; *Bacillus licheniformis* ~3 $\mu mol/g_{CDW}$ [Bierbaum et al., 1991]). Other nucleotide concentrations were 7.7 $\mu mol/g_{CDW}$ (UTP), 3.5 $\mu mol/g_{CDW}$ (GTP), and 3.9 $\mu mol/g_{CDW}$ (CTP) (see Figure 2). Levels for G-6-P, F-6-P, and F-1,6-bP were 6.5, 10.7, and 3.0 $\mu mol/g_{CDW}$, respectively.

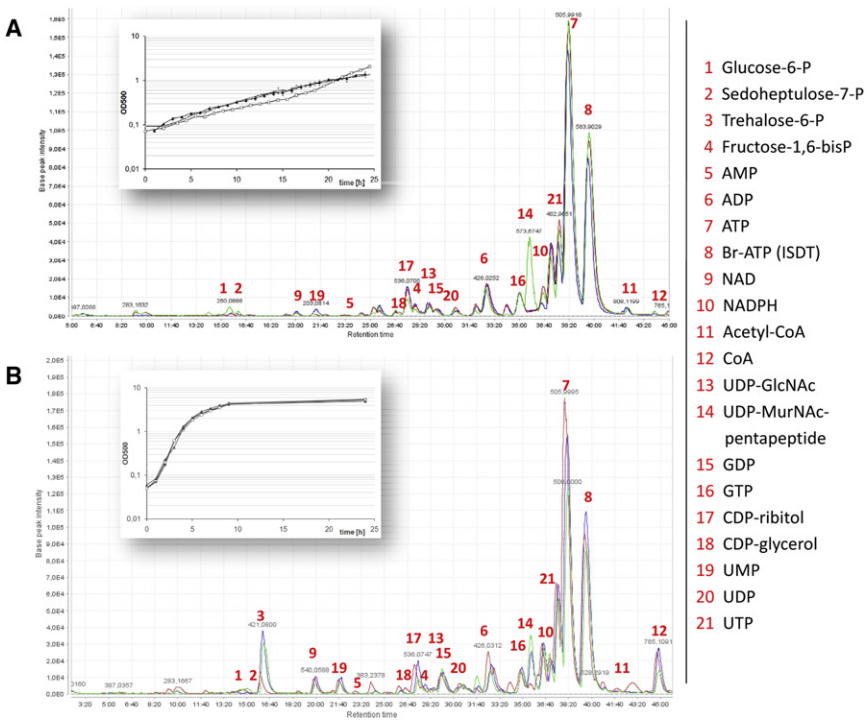

Figure 1. Overlay of Raw LC/MS Base Peak Chromatograms of Representative Samples from *S. aureus* 8325 Wild-Type (blue), Kinase Deletion Mutant Δ*pknB* (red), and Phosphatase Deletion Mutant Δ*stp* (green)

Cells were grown in (A) chemical defined medium and (B) in complex LB medium (all sampled at $OD_{500/540}$ 1.0, exponential growth). Profiles display negative ESI mode MS acquisitions with x axis: retention time (min) and y axis: peak height (signal intensity). Twenty identified compounds are shown as examples. (insets) Growth of *S. aureus* 8325 wild-type (◇), kinase deletion mutant Δ*pknB* (□) and Δ*stp* (▲) in each medium, respectively.

The overall energy metabolite levels for CDM-grown cells were comparable to those from LB, with only GXP levels significantly lower in CDM-derived cells. This may be due to the lack of guanosine in CDM, in contrast to LB medium which contains purines and pyrimidines (Sezonov et al., 2007). On the other hand, IMP and AXP levels were slightly higher in CDM, demonstrating a branching off from GXPs (for more data, see Figure 2; Table S1). Differences in concentration of amino acids, fatty acids, and other compounds between the two media indicated metabolome alterations driven by different anabolite availability (M. Liebeke and M. Lalk, unpublished data). Other differences were also recorded, e.g., trehalose-6-P was only present in cells grown in LB medium. UDP-sugar-derived cell wall precursors were more abundant in LB broth, indicating a complex saccharide content of LB medium as presumed earlier (Hanko and Rohrer, 2000). Overall, the LC-MS method presented achieved robust and accurate metabolite data, with a usually technical error range in metabolomics around 5%–20% (Kose et al., 2007). Metabolites with a fast turnover like nucleotides (e.g., ATP, UTP) or redox-sensitive ones (e.g., NADH) showed higher errors in the biological samples in agreement with previous results (van der Werf et al., 2008)

Alteration of Metabolites during Growth

In order to determine growth-dependent changes in metabolite levels, we analyzed LB-grown wild-type and mutant populations harvested at exponential, mid-exponential, and late-exponential growth phase. Hierarchical cluster analysis of metabolite levels in the wild-type resulted in three major clusters. These were 1) metabolites that increased with culture age (*Cluster 1*; e.g., AMP, adenylsuccinate, CoA), 2) metabolites that decreased with culture age (*Cluster 3*; e.g., G-6-P, GTP, acetyl-CoA, UDP-MurNAc-A-E), and 3) metabolites that show no change (*Cluster 2*; e.g., FAD, UMP) (see Figure S1). The majority of energy-rich and glycolysis-dependent metabolites decreased over time. Cell wall precursors behaved in the same way, indicating that the cytosolic pool of complex, energy-rich metabolites is diminished and initiates entry into stationary phase.

Comparisons of *S. aureus* Metabolites in Wild-Type and Serine/Threonine Kinase and Phosphatase Mutant Cells

The *pknB* and *stp* deletion mutants grew almost as the wild-type in both CDM and LB medium. The *pknB* mutant displayed a somewhat lower growth rate but higher final yield (see Figure 1, insets). A comprehensive list of compounds present in exponential phase wild-type and both mutants was compiled by combination the targeted (focus on nucleotides) and untargeted metabolite search; visualization of the results was done by heat map plotting. In general, metabolites reflecting the energy states did not differ substantially for wild-type, Δ*pknB* and Δ*stp* cells. A few significant differences between wild-type and mutant strains were observed in LB medium (see heat map in Figure 3). Considering the similarity between growth curves, this observation is not surprising because the cells have to keep their energy state in balance for successful growth. The specific differences in metabolite concentrations are discussed within their corresponding pathway contexts below.

Central Carbon Metabolism

For *S. aureus* growing in complex medium, glycolysis intermediates underwent time-dependent changes. There was a clear correlation between glucose-6-P, fructose-6-P and fructose-1,6-bisP consumption up to stationary phase, and an ATP decrease coupled with ADP/AMP increase in all strains, indicating nutrient limitation. PknB reportedly causes the phosphorylation of fructose-1,6-bisphosphate aldolase (FbaB), which degraded fructose-1,6-bisP to glycerinealdehyd-3-P and

Table 1. List of Detected Metabolites in *S. aureus* Wild-Type Cells Grown in LB Medium

Metabolite	KEGG Entry	Metabolite	KEGG Entry	Metabolite	KEGG Entry
Adenosine	C00212	IMP	C00130	Erythrose-5-P	C00279
AMP	C00020	IDP	C00104	Sedoheptulose-7-P	C05382
ADP	C00008	ITP	C00081	Sedoheptulose-1,7-bisP	C00447
ATP	C00002	CMP	C00055	Glucose-6-P	C01172
dAMP	C00360	CDP	C00112	Fructose-6-P	C05345
dADP	C00206	CTP	C00063	Fructose-1,6-bisP	C05378
dATP	C00131	dCMP	C00239	Riboflavin	C00255
ADP-ribose	C00301	dCDP	C00705	NAD^+	C00003
Adenylsuccinate	C03794	dCTP	C00458	NADH	C00004
c(3,5)AMP	C00575	CDP-glycerol	C00513	$NADP^+$	C00006
Guanosine	C00387	CDP-ribitol	C00789	NADPH	C00005
GMP	C00144	Xanthosine	C01762	FAD	C00016
GDP	C00035	XMP	C00655	FMN	C00061
GTP	C00044	2-dTMP	C00364	CoA	C00010
dGMP	C00362	2-dTDP	C00363	Acetyl-CoA	C00024
dGDP	C00361	2-dTTP	C00459	Succinyl-CoA	C00091
dGTP	C00286			Malonyl-CoA	C00083
cyclic-(3,5)-GMP[a]	C00942			Butyryl-CoA	C00136
cyclic-di-GMP[a]	C16463			GSH[a]	C00051
ppGpp[a]	C01228			5-Phosphoribosylamine	C03090
(p)ppGpp[a]	C04494			GAR	C03838
GDP-glc	C00394			FGAR	C04376
Uridine	C00299			SCAIR	C04823
UMP	C00105			AICAR	C04677
UDP	C00015			PRPP	C00119
UTP	C00075				
dUMP	C00365				
dUDP	C01346				
dUTP	C00460				
UDP-Glc	C00029				
UDP-GlcNAc	C00043				
UDP-GlcNAcEP	C04631				
UDP-MurNAc	C01050				
UDP-MurNAc-A	C01212				
UDP-MurNAc-A-E	C00692				
UDP-MurNAc-A-E-L	C04700				
UDP-MurNAc-A-E-L-A-A	C04846				
Undecaprenol-P	C00348				

All identified compounds listed here were confirmed by pure chemical standards. Synonyms of metabolites, measured m/z ratios and retention times, are given in detail in Table S1.

[a] Metabolites that were detected by the IP-LC/MS method from an artificially mixture to illustrate the detection spectrum of the chosen method.

glycerone-P (Lomas-Lopez et al., 2007). We observed a significant decrease in the levels of fructose-1,6-bisP level and its precursors G-6-P and F-6-P in the phosphatase (Δ*stp*) mutant, resulting in decreased values for compared to wild-type (see Figure 3). In contrast, FbaA is reportedly upregulated 1.5-fold in the Δ*pknB* strain (Donat et al., 2009). This upregulation is possibly a compensation for decreased activity caused by a lack of phosphorylation or by a higher outflow into other pathways. Presumably, the Δ*stp* mutant has a stronger FbaB enzyme activity and therefore increased glycolysis activity than the wild-type. In LB medium with a peptide/amino acid-rich content and low glucose levels, the deletions clearly have no effect on the growth phenotype. No differences were found in extracellular amounts of overflow metabolites from glycolysis, such as acetic acid, or in medium compounds between the mutants and the wild-type cultures (see Figure S4).

Table 2. Optical Density and Calculated Adenylate Energy Charge of *S. aureus* Cell Suspension for Wild-Type and Serine/Threonine Kinase Deletion Mutant (Δ*pknB*) and Phosphatase Deletion Mutant (Δ*stp*) in Two Different Growth Media

Growth Medium	*S. aureus* 8325	Optical Density at Sample Time ($OD_{500/540}$ ± SD[a])	Energy Charge (EC ± SD[a])]
CDM	wt	1.004 ± 0.01	0.882 ± 0.004
	Δ*pknB*	1.010 ± 0.01	0.891 ± 0.014
	Δ*stp*	1.000 ± 0.00	0.921 ± 0.004
LB	wt	1.004 ± 0.01	0.876 ± 0.035
	wt	2.613 ± 0.06	0.849 ± 0.033
	wt	3.003 ± 0.01	0.744 ± 0.099
	Δ*pknB*	1.010 ± 0.01	0.874 ± 0.032
	Δ*pknB*	2.227 ± 0.03	0.840 ± 0.052
	Δ*pknB*	3.110 ± 0.01	0.733 ± 0.105
	Δ*stp*	1.000 ± 0.00	0.893 ± 0.025
	Δ*stp*	2.610 ± 0.02	0.831 ± 0.065
	Δ*stp*	3.203 ± 0.00	0.751 ± 0.109

Chemical defined medium, CDM, OD_{500}; complex medium, LB, OD_{540}
[a] SD of results from three independent cultivations.

Another central pathway in carbon metabolism is the tricarbonic acid cycle (TCA) (our method detected succinyl-CoA, acetyl-CoA and CoA) formed in that pathway. It has been shown that OdhB (dihydrolipoamide succinyltransferase) is upregulated 2.4-fold in the Δ*pknB* mutant (Donat et al., 2009), but no significant changes were detected for succinyl-CoA or its precursor CoA in Δ*pknB* cells. The Δ*stp* mutant had reduced levels of both metabolites compared with wild-type. This may be due to a shift in the glycolysis crossroads. For example, F-6-P outflow for synthesis of amino sugars required for cell wall biosynthesis is reduced in the *stp* mutant, described below. Phosphate acetyl transferase (Pta) is a phosphorylated protein in *S. aureus* (Lomas-Lopez et al., 2007), but deletion of *pknB* or *stp* was not associated with significant alterations in CoA and acetyl-CoA levels. This may be due either to a different phosphorylation mechanism for Pta or because phosphorylation is not essential for its function.

Nucleotide Metabolism in *S. aureus*

The synthesis of a tremendous variety of precursors and macromolecules is dependent on folate metabolism, which serves as a methyl-group donor in pyrimidine and purine synthesis and therefore in biosynthesis of nucleotides, DNA, RNA, and some amino acids (Figure 3A). Compounds quantified in *S. aureus* are indicated in the metabolite list (Table 1). The methyl group donor 10-formyl-THF was detected only in trace amounts in all samples. Nevertheless it plays a key role in AXP and GXP synthesis but not in UXP or CXP synthesis. The nucleoside precursors of these nucleotides show poor ionization feasibility in our negative mode MS method, and therefore fall below the detection limit. The main pathway for synthesis of adenosine and guanosine phosphates is de novo synthesis from 5-phosphoribosylamine, starting with ribose-5-P and PRPP, which, in turn, is derived from the pentose-phosphate pathway by transferring an amino group from glutamine via amidophosphoribosyltransferase (PurF). We were able to detect most of the intermediate metabolites of the purine pathway, except 5-P-ribosylamine, FGAM, CAIR, and FAICAR. This may be due to high enzyme activities or one-sided equilibrium of a reaction, which leads to low levels of the affected metabolites. A slight decrease in the above mentioned and detected metabolites was observable in Δ*stp* cells compared to wild-type (Figure 3C).

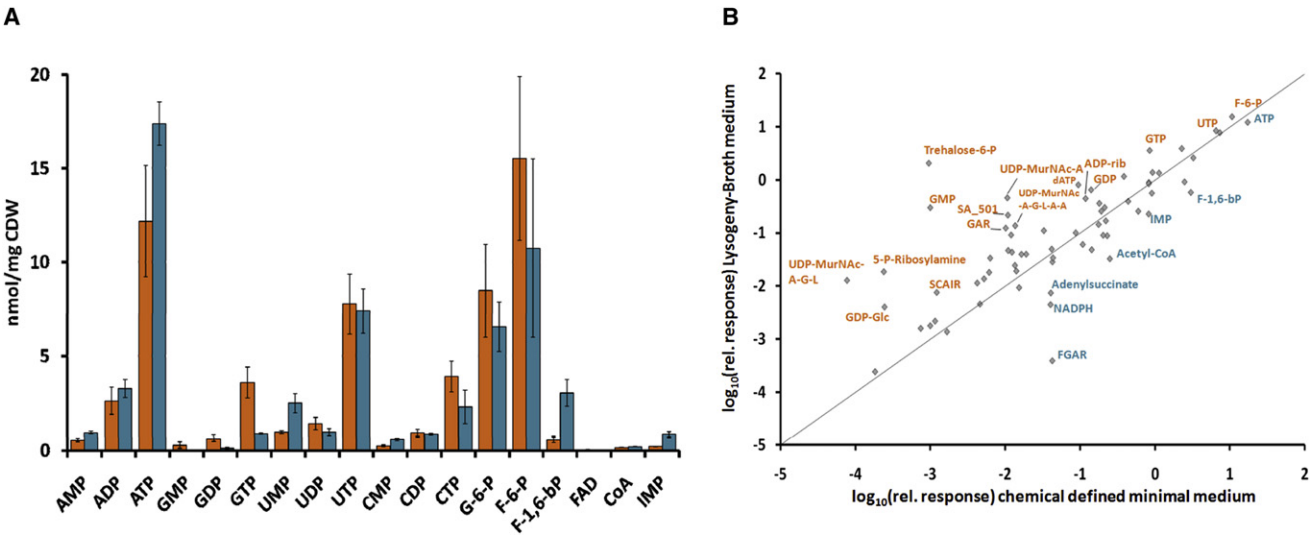

Figure 2. Absolute Metabolite Concentrations of *S. aureus* Cells Grown in Different Media

(A) Selected absolute intracellular metabolite concentrations of *S. aureus* 8325 wild-type normalized to cell dry weight (CDW) at exponential growth phase (OD_{540} = 1.0) in complex LB medium (orange bars) and minimal CDM medium (blue bars) as quantified by IP-LC-MS (error bars representing SD of results from three independent cultivations). Abbreviations for metabolites are in Table S1.

(B) Plot of correlated metabolite signal areas from cells grown in LB (y axis) and CDM (x axis). The diagonal line within the correlation plot is the ideal 1:1 graph of cells grown in LB versus CDM. Metabolites with at least 3-fold change are marked. The log_{10} values of corrected areas (internal standard and optical density) are plotted, taking into account the differences in amount between the detected metabolites. See also Figure S1.

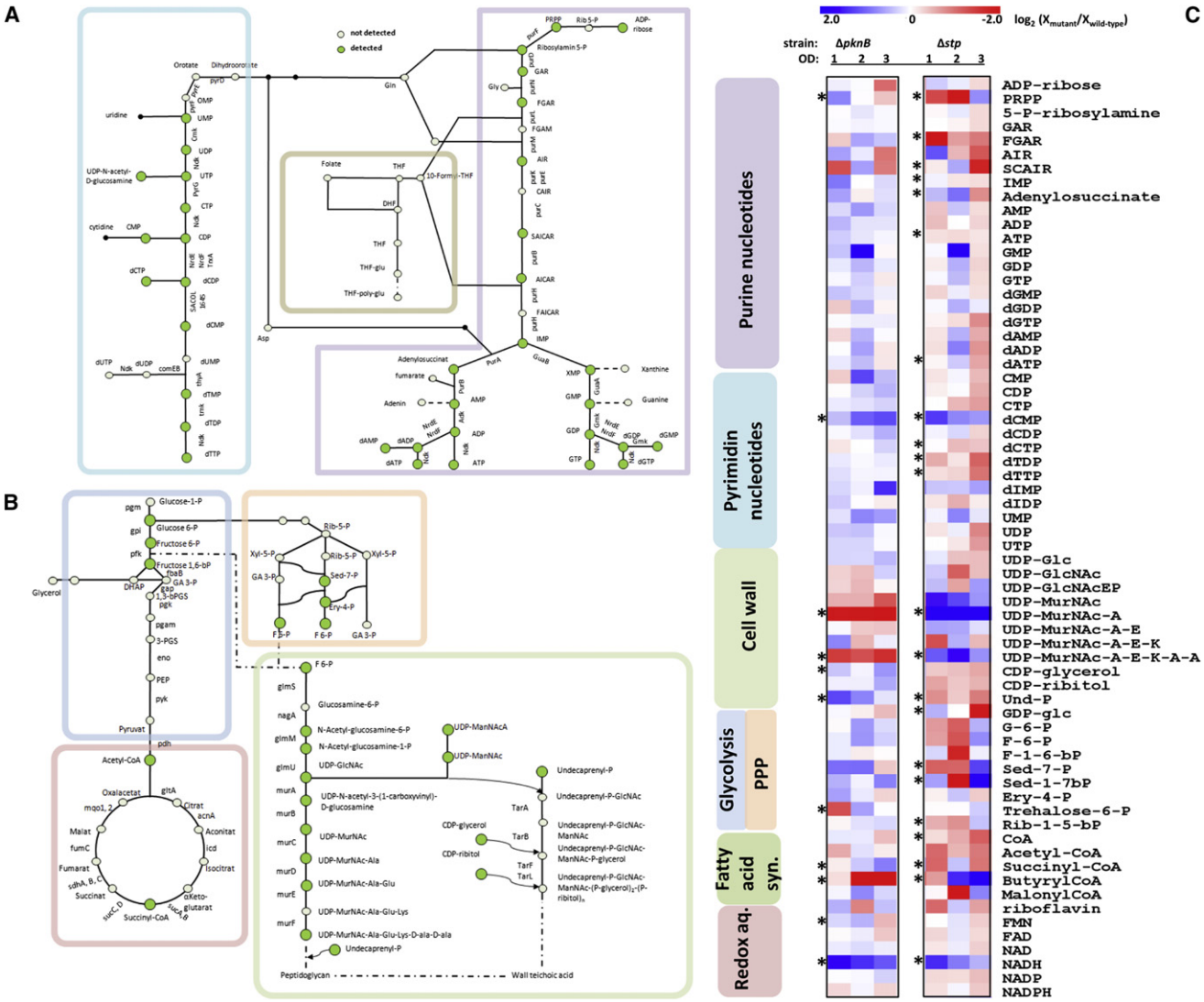

Figure 3. Analyzed Pathways of *S. aureus*

Metabolic pathways of *S. aureus*, (A) purine and pyrimidine nucleotide synthesis, folate metabolism, and (B) glycolysis, pentose-phosphate pathway, tricarbonic acid cycle, cell wall precursor synthesis. (C) Profiles of intracellular metabolites of *S. aureus* Δ*pknB* and Δ*stp* mutant compared each to parent wild-type strain (color coded by values of $\log_2 [X_{mutant}/X_{wild\text{-}type}]$ when harvested at different growth stages [exponential, mid-, and late exponential growth phase; $OD_{540} = 1, 2, 3$]). Metabolite profiles were ordered after occurrence in respective metabolic pathways (A) and (B). Significant alterations (Student's two-tailed t test $p < 0.1$) are marked with an asterisk. Abbreviations for metabolites and enzymes are in Table S1.

Phosphorylation of PurA, adenylosuccinate synthetase by PknB, serves to decrease the activity of this enzyme in *S. aureus* in vitro (Donat et al., 2009). This final step in purine-nucleotide synthesis leads to the formation of AMP from IMP via adenylosuccinate. Our in vivo results mirror the PknB dependant decrease in activity as the *pknB* mutant contained elevated AMP, ADP, and ATP concentrations in the stationary phase, reflecting increased adenylosuccinate levels. In contrast, *stp* deletion led to decreased levels of these metabolites, which may be caused by decreased de-phosphorylation of PurA due to a lack of STP. Guanosine phosphates showed no variations between the tested strains. The effect on metabolite alterations was not as drastic as assumed after analyzing the transcriptome data. Therefore, it seems not only to be a phosphorylation and dephosphorylation influence on PurA activity by PknB/STP, indicating an alternative activation/deactivation mechanism for PurA in our *S. aureus* strain.

Even though Debarbouille et al. (2009) show that the addition of adenine to a *S. aureus* Stk1 mutant in RPMI medium decompensates the growth deficiencies without this precursor, no significant differences in levels of AXP were observed between the CDM used in this work (nucleoside free) and complex LB medium. This may be due to the IMP directed synthesis of AXPs (see Figure 3). All intermediates in pyrimidine metabolism, with orotate from aspartate and carbamoyl-P, were detected using the presented method, with the exception of dUXPs and OMP, which were not detected in our sample set. Levels of CXPs and UXP were not significantly altered in Δ*pknB* compared

with wild-type. On the other hand, Δ*stp* shows significantly decreased levels of UTP and CTP in late growth phase.

Cell Wall Synthesis

Cell wall precursors such as UDP-N-acetylmuramate (UDP-MurNac), UDP-MurNac-Ala, and UDP-MurNAc-Ala-Glu for peptidoglycan synthesis, as well as UDP-N-acetylglucoseamine (UDP-GlcNAc) for wall teichoic acid synthesis (Weidenmaier and Peschel, 2008), were detected in notable amounts in all tested strains and under all conditions (see Figure 3B). These important building blocks are derived from the glycolysis intermediate F-6-P and glucoseamine-1-P. Their synthesis is tightly regulated (Komatsuzawa et al., 2004) and we can see clear differences between both mutants and the wild-type. MurQ (N-acetylmuramic acid 6-phosphate etherase), producing Glc-NAc-6-P from Mur-NAc-6-P, is downregulated in Δ*stp* (0.19-fold) (S.D. and K.O., unpublished data), indicating a lower demand for Glc-NAc-6-P in Δ*stp* for petidoglycan synthesis.

Genes for cell envelope, especially cell wall metabolism were upregulated 1.5- to 4.1-fold in the Δ*pknB* mutant (Donat et al., 2009). For example *murZ* (*murA*) is increased 1.5-fold. It encodes for UDP-N-acetylglucoseamine-1-carboxyvinyl-transferase-2, catalyzing the conversion of UDP-GlcNAc to UDP-N-acetyl-3-(1-carboxyvinyl)-D-glucosamine. Intracellular UDP-GlcNAc decreased 2.5-fold in the kinase mutant and also slightly decreased in the phosphatase mutant compared to the wild-type cells. The next step in peptidoglycan synthesis, regulated by MurA and MurB, is the formation of UDP-MurNAc. The two tested mutants showed opposite levels of UDP-MurNAc: *S. aureus* Δ*pknB* has lower (0.5-fold) and Δ*stp* higher concentrations (2.1-fold) compared with the wild-type. This coincides with the decrease/increase in downstream metabolites in this pathway via UDP-N-Acetylmuramic acid:L-alanine ligase (MurC) to UDP-MurNAc-Ala (0.2 versus 5.0-fold) and L-glutamine ligase (MurD) to UDP-MurNAc-Ala-Glu (0.8 versus 1.4-fold) (see Figure 3C).

It has recently been shown that the activity of MurC in *Corynebacterium glutamicum* depends on serine/threonine kinase (PknA) activity (Fiuza et al., 2008). In fact, to validate the importance of these targets for new active antibiotic compounds, the development of inhibitors to MurC or MurD has been pursued (Sink et al., 2008). The preliminary steps before anchoring to undecaprenylphosphate are catalyzed by MurE and MurF. Interestingly, UDP-MurNAc-Ala-Glu-Lys was only detected in trace amounts but UDP-MurNAc-Ala-Glu-Lys-D-Ala-D-Ala was found in higher abundance with a 2.1-fold increase in the Δ*stp* mutant and a 0.39-fold decrease in Δ*pknB* under both growth conditions. This molecule constitutes the end of the cytoplasmic steps in peptidoglycan synthesis, and we were able to account for all biosynthetic steps up to this one with our method. Studying the membrane associated binding of lipid II to the UDP-pentapeptide moiety and glycine cross linkage (Schneider et al., 2004) is so far not possible with our method. A transcriptional downregulation of *lytM* (peptidoglycan hydrolase) in Δ*pknB* (1.7-fold) was observed, possibly to prevent further decrease in cell wall thickness. In Δ*pknB* an upregulation of *vraS* and *vraR* (2.5-fold) has been reported (Donat et al., 2009). These genes have been described as part of a two component system for sensing peptidoglycan damage and coordinating a damage response (Belcheva and Golemi-Kotra, 2008). This also hints at altered PG synthesis in this deletion strain.

Nucleotides (CTP) and deoxynucleotides were much decreased in late exponential phase *stp* mutant cells, due perhaps to extensive production of UDP-derivatives for cell wall synthesis. To summarize the above results, they support a key role of the serine/threonine kinase/phosphatase system in *S. aureus* peptidoglycan metabolism. These data confirm phenotypic observations, where *pknB* deletion leads to increased fosfomycin resistance (fosfomycin is a MurA inhibitor; Blake et al., 2009). In the absence of PknB-dependent activation, the resulting reduction in pathway activity probably results in decreased susceptibility to fosfomycin. Unless cell wall synthesis is altered, an increased lysing activity by the detergent Triton X-100 (Donat et al., 2009) is suspected. Vice versa, deletion of the corresponding phosphatase leads to higher cell wall precursor concentrations, a thicker cell wall, and decreased activity of lysostaphin and cell wall synthesis targeting antibiotics (Beltramini et al., 2009).

Other important cell wall glycopolymers in Gram-positive bacteria are the wall teichoic acids (WTAs). They play a major role in host-cell interactions for pathogens like *S. aureus* (Weidenmaier and Peschel, 2008). WTAs are produced from UDP-GlcNAc, ManNAc, CDP-glycerol, and CDP-ribitol to form block glycopolymers of GlcNAc-ManNAc. The result is a peptidoglycan linker with long phosphoribitol and shorter phosphoglycerol repeats (Brown et al., 2008). CDP-glycerol and CDP-ribitol the main precursors for WTA, displayed altered abundance in the mutants. They show contrary levels compared with peptidoglycan precursors in respective mutants. We observed increased levels of CDP-glycerol/-ribitol (1.5-fold) in the Δ*pknB* mutant and decreased levels in the Δ*stp* mutant (0.5-fold). Similar modulation was observed at the transcriptional level as *rbsD* and *rbsU* (ribose permease/transporter) are upregulated in Δ*pknB* (1.7/1.9-fold), perhaps to support the CDP-ribitol pool in the kinase mutant. The only shared metabolite for both pathways is the membrane anchor undecaprenyl-phosphate (Und-P), which is increased in Δ*pknB* (1.7-fold) and decreased in Δ*stp* (0.6-fold) (Figure 4). As recently shown by D'Elia et al. (2009), a genome context interaction between peptidoglycan, isoprenoid and teichoic acid biosynthesis exists for *B. subtilis*. Our in vivo metabolite measurements provide additional support for a correlation between WTA and PG precursor concentrations in *S. aureus*. Taken together, these results from peptidoglycan precursor concentrations show that PknB/STP influences *S. aureus* cell wall metabolism in a key manner. These findings may help to establish new routes to antimicrobial therapy. The selective inhibition of PknB or STP could provide a new basis for antibiotic action. Moreover, deletion of PknB leads to a decreased bacterial load in a mouse infection model (Debarbouille et al., 2009). We speculate that this weakened defense is due to an altered cell wall structure with lower peptidoglycan content and more WTA precursors, therefore an important link to virulence by serine/threonine kinases in staphylococci.

DISCUSSION

Cell wall biosynthesis in Gram-positive bacteria such as *S. aureus* is a highly regulated process. Transcriptomic data

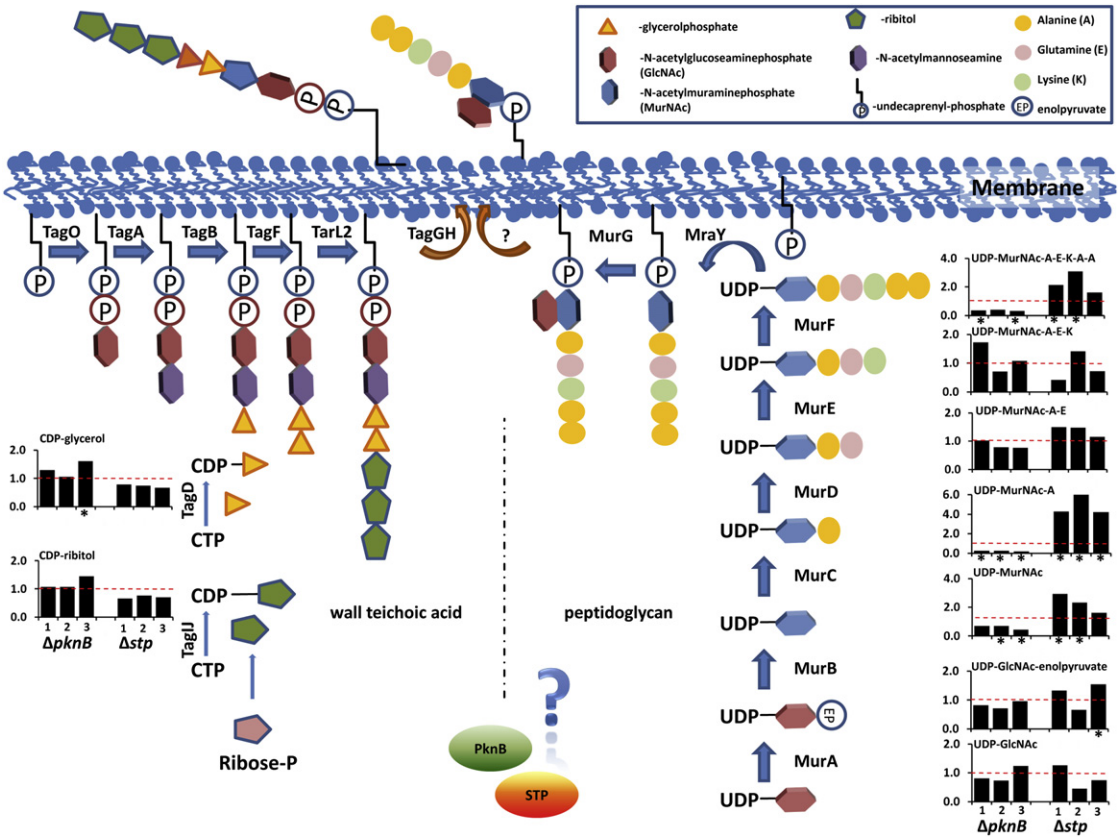

Figure 4. Wall Teichoic Acid and Peptidoglycan Synthesis in *S. aureus*

Bar charts represent the fold changes of respective metabolites from Δ*pknB*/Δ*stp* deletion mutants compared with wild-type cells (red line) at different growth stages (exponential, mid-, and late exponential growth phase; OD_{540} 1, 2, and 3). Significant alterations (Student's two-tailed t test $p < 0.1$) are marked with an asterisk under the bar chart (error bars representing SD of results from three independent cultivations). Abbreviations for metabolites and enzymes are in Table S1. Biochemical nomenclature was chosen according to Xia and Peschel (2008).

have suggested a key role for regulation of precursor biosynthesis rates. Here, we present the first metabolomic approach to analyze intracellular metabolites of *S. aureus*, using a newly developed analytical procedure based on a unique extraction protocol followed by the presented IP-LC/MS. Using this approach, we were able to study a large selection of metabolites as affected by the kinase PknB and the phosphatase Stp. Even thought hundreds of mass spectral tags were determined, we focus on identified metabolites (identification by comparison with pure chemical standards; Sumner et al., 2007). Nevertheless, it has now been possible to decipher abundances for *S. aureus* nucleotide metabolism, parts of the main carbon flux pathways like glycolysis, pentose phosphate pathway, and, important for bacteria with a host competitive lifestyle, the cell wall precursors synthesis.

Culture medium (CDM or LB) did not affect nucleotide and cell wall precursor levels much, indicating that these metabolites are under rigorous regulation and need to maintain a constant level in living cells. Some other metabolites, such as trehalose-6-P and GXP, were affected by the medium components. Medium composition and growth conditions must therefore be defined clearly to enable network reconstructions and other bioinformatic approaches of published metabolite values. This also holds for growth phase-dependent alterations on the metabolome level, which have to be handled with care by comparing data from different studies based on various experimental setups.

Interestingly, the effects of deletion of *pknB* and *stp* fold-alteration in nucleotide or cofactor pools were not drastic as indicated by a previous transcriptomic study (Donat et al., 2009). These results are consistent with similar growth phenotypes, because most of the metabolites like ATP or NADH are major players in the bacterial metabolome. A more drastic effect of growth can be assumed for disturbances in the central pathways through the deletion of *pknB* or *stp*. However, a clear dependence of cell wall synthesis on PknB/STP was found, indicating a new regulatory mechanism for this system. At the metabolite level, there is clear evidence for the involvement of PknB/STP in peptidoglycan biosynthesis. There also appears to be a preference for MurB/C and MurF, considering the strong changes in the dependent metabolites (see Figure 4). These enzymes and others in this pathway are probably activity-regulated by dephosphorylation and phosphorylation, as has been described for other microorganisms (Fiuza et al., 2008; Novakova et al., 2005; Parikh et al., 2009). In the future, detailed in vitro and in vivo protein phosphorylation studies to elucidate

phosphorylation sites and in vivo enzyme activities of PknB/STP will follow.

An involvement of PknB/STP in wall teichoic acid and peptidoglycan balance is feasible when considering 1) altered resistance to antibiotics, 2) decreased susceptibility against cell wall attacking substances, and 3) the metabolome data reported here. The effects of *stp* deletion are more drastic than for *pknB* deletion, indicating an additional kinase in *S. aureus* 8325 which may compensate for such disturbances.

SIGNIFICANCE

This report provides detailed information about the metabolome of *S. aureus* and reveals disturbances in staphylococcal metabolism through genetic deletions of serine/threonine kinase and phosphatase. In particular, the impact of these enzyme systems on the cell wall metabolome is shown for the first time and significant alterations were observed. We have demonstrated that the LC/MS method described is a powerful tool for investigations into bacterial physiology. In addition to recent transcriptome approaches and phenotypic screenings to the impact of phosphorylations in *S. aureus* through PknB, our results not only verify protein targets like PurA, but also provide evidence for possible new ones. The metabolome data strongly indicate an alteration in peptidoglycan synthesis, mainly involving the enzymes MurB/C and MurF. Metabolomics reveals corresponding and additional information as generated with transcriptome analysis by Donat et al. (2009) for the Δ*pknB* strain. Metabolome analysis is another sophisticated postgenomic technique to elucidate the impact of protein phosphorylation in bacteria. This is to our knowledge the first description of metabolome profiles in phosphoproteome altered bacterial cells.

Finally, the presented bioanalytical method is also suitable for analyzing other mutant strains or to investigate stress adaptations, e.g., in mechanism of action studies of new antibiotics against *S. aureus* and other pathogens resistant to antibiotics.

EXPERIMENTAL PROCEDURES

Bacterial Strains and Growth Conditions

Staphylococcus aureus 8325 and its isogenic eukaryotic-type kinase deletion mutant (Δ*pknB*) (Donat et al., 2009) and protein phosphatase deletion mutant (Δ*stp*) (S.D. and K.O., unpublished data) were cultured at 37°C and 220 rpm to an OD_{500} of 1.0 in 100 ml chemical defined medium (CDM) (Meyer et al., 2010) and in 100 ml lysogeny broth (LB) (Bertani, 2004) medium (Sigma-Aldrich) to an OD_{540} of 1.0, 2.0, and 3.0 (in 500 ml shaking flasks), respectively (Donat et al., 2009).

Sample Procedure and Metabolite Extraction

Samples for intracellular metabolome analysis were obtained by harvesting cells on 0.45 μm filters connected to vacuum, as described previously for a *B. subtilis* metabolome study (Liebeke et al., 2008) and recently examined in depth for *S. aureus* (Meyer et al., 2010). Cells were washed immediately on the filter with isotonic cooled NaCl solution (0.6%; <4°C) and subsequently quenched with an ethanol/water solution (60/40 wt/vol (<4°C) and liquid nitrogen and stored at −80°C until further processing. All following procedures were performed on ice. After thawing of the cell suspension and incorporated filter, the mixture was mixed ten times to remove cells from the filter and destroy the filter by shaking. Quenching solution and cells were transferred to glass bead filled tubes. Metabolite extraction was performed by disruption of cells in a Ribolyzer, and cell debris was removed by centrifugation (8500 rpm and 5 min, 4°C). Supernatants were pooled after an additional washing step of the glass beads and frozen at −80°C until lyophilization. Samples were dried and prepared as described previously (Liebeke et al., 2008). The problem of leakage in this sampling protocol is excluded by the continuous use of the same solution for quenching and extraction.

IP-LC/MS Conditions

Detection of metabolites was performed by IP-LC/MS. The system consisted of an Agilent liquid chromatographic System 1100 (Agilent Technologies) equipped with a quartany pump, an online degasser, and an autosampler. The LC was coupled to a micrOTOF (Bruker, Rheinstetten) operating in electrospray negative ionization, full scan mode, and the mass range was set to 100–2000 Da at a resolution of 10,000 (at m/z 1033). Source parameters were as follows: drying gas (N_2) flow rate, 8.0 l/min; drying gas temperature, 180°C; nebulizer, 1.6 bar (160 kPa); capillary voltage, 4500 V; skimmer 1 voltage, −50 V; skimmer 2 voltage, −24 V. Reference masses of compounds from Agilent tune mix for electro spray applications in negative mode with empirical formulas 112.99, 431.98, 601.98, 1033.99, 1633.95, 2233.91, and 2833.87 were used for automated tuning in each chromatographic run. Dried samples were dissolved in 100 μl aqua destillata prior to injection and centrifuged for 2 min (13,000 rpm, 2°C). The supernatant was transferred into glass vials and then placed into the autosampler. Chromatographic separation was performed at 25°C using a RP-C18 (150 × 4.6 mm, 3.5 μm) Waters Symmetry-Shield column connected to a C18 Waters precolumn. The mobile phase was A (5% methanol and 95% water, containing 10 mM tributylamine as ion-pairing reagent and acetic acid for pH adjustment to pH 4.8) and B (100% methanol). The gradient elution started with 100% A for 2 min, 0%–20% B in 2 min, 20%–31% B in 11 min, 31%–60% B in 19 min, 60%–100% B in 5 min, hold 100% B for 15 min, 100%–0% B in 6 min, and hold 3 min at 0% B. The gradient flow rate was 0.3 ml/min. For equilibration of the column, a 5 min prerun with initial gradient conditions was performed before each sample.

Quantitative Metabolite Analysis and Chemicals

Generation of quantitative metabolite data and information about chemicals used are in Supplemental Experimental Procedures.

Extracellular Metabolite Profiling by ^{1}H-NMR

Detection and determination of extracellular metabolites was carried out according to Liebeke et al. (2009). For detailed description, see Supplemental Experimental Procedures and Figure S4.

Metabolite List Processing and Statistics

All acquired IP-LC/MS chromatograms from *S. aureus* samples were evaluated by the freely available software MZmine (Katajamaa et al., 2006). Obtained peak lists were evaluated for identified metabolites and imported to Multi experiment viewer (TMV4 viewer) (Saeed et al., 2003). Hierarchical cluster analysis (HCL) was performed using optical density normalized metabolite values, each calculated as percentage of highest level across growth. For detailed parameters for all software used, see Supplemental Experimental Procedures.

SUPPLEMENTAL INFORMATION

Supplemental Information includes Supplemental Experimental Procedures, four figures, and one table and can be found with this article online at doi:10.1016/j.chembiol.2010.06.012.

ACKNOWLEDGMENTS

We are grateful to K. Dörries for creating parts of the metabolite list, and to H.-G. Sahl and U. Dobrindt for providing UDP-MurNAc-peptides and c-di-GMP. This work was supported by grants from the Deutsche Forschungsgemeinschaft (SFB/TRR34, La1289/2-1), the Bundesministerium für Bildung und Forschung (BMBF, ZIK-FunGene), and the state of Mecklenburg-Vorpommern (UG07068). M.Li. is a recipient of a fellowship from the Alfried Krupp von

Bohlen and Halbach-Stiftung: "A Functional Genomics Approach in Infection Biology."

Received: December 7, 2009
Revised: June 24, 2010
Accepted: June 28, 2010
Published: August 26, 2010

REFERENCES

Atkinson, D.E. (1968). The energy charge of the adenylate pool as a regulatory parameter. Interaction with feedback modifiers. Biochemistry *7*, 4030–4034.

Bajad, S.U., Lu, W., Kimball, E.H., Yuan, J., Peterson, C., and Rabinowitz, J.D. (2006). Separation and quantitation of water soluble cellular metabolites by hydrophilic interaction chromatography-tandem mass spectrometry. J. Chromatogr. A *1125*, 76–88.

Becker, K., Bierbaum, G., von Eiff, C., Engelmann, S., Gotz, F., Hacker, J., Hecker, M., Peters, G., Rosenstein, R., and Ziebuhr, W. (2007). Understanding the physiology and adaptation of staphylococci: a post-genomic approach. Int. J. Med. Microbiol. *297*, 483–501.

Becker, S.A., and Palsson, B.O. (2005). Genome-scale reconstruction of the metabolic network in Staphylococcus aureus N315: an initial draft to the two-dimensional annotation. BMC Microbiol. *5*, 8.

Belcheva, A., and Golemi-Kotra, D. (2008). A close-up view of the VraSR two-component system: a mediator of staphylococcus aureus response to cell wall damage. J. Biol. Chem. *283*, 12354–12364.

Beltramini, A.M., Mukhopadhyay, C.D., and Pancholi, V. (2009). Modulation of cell wall structure and antimicrobial susceptibility by a Staphylococcus aureus eukaryote-like serine/threonine kinase and phosphatase. Infect. Immun. *77*, 1406–1416.

Bertani, G. (2004). Lysogeny at mid-twentieth century: P1, P2, and other experimental systems. J. Bacteriol. *186*, 595–600.

Bierbaum, G., Giesecke, U.E., and Wandrey, C. (1991). Analysis of nucleotide pools during protease production with *Bacillus licheniformis*. Appl. Microbiol. Biotechnol. *35*, 725–730.

Blake, K.L., O'Neill, A.J., Mengin-Lecreulx, D., Henderson, P.J., Bostock, J.M., Dunsmore, C.J., Simmons, K.J., Fishwick, C.W., Leeds, J.A., and Chopra, I. (2009). The nature of Staphylococcus aureus MurA and MurZ and approaches for detection of peptidoglycan biosynthesis inhibitors. Mol. Microbiol. *72*, 335–343.

Brown, S., Zhang, Y.H., and Walker, S. (2008). A revised pathway proposed for Staphylococcus aureus wall teichoic acid biosynthesis based on in vitro reconstitution of the intracellular steps. Chem. Biol. *15*, 12–21.

Cordell, R.L., Hill, S.J., Ortori, C.A., and Barrett, D.A. (2008). Quantitative profiling of nucleotides and related phosphate-containing metabolites in cultured mammalian cells by liquid chromatography tandem electrospray mass spectrometry. J. Chromatogr. B Analyt. Technol. Biomed. Life Sci. *871*, 115–124.

Coulier, L., Bas, R., Jespersen, S., Verheij, E., van der Werf, M.J., and Hankemeier, T. (2006). Simultaneous quantitative analysis of metabolites using ion-pair liquid chromatography-electrospray ionization mass spectrometry. Anal. Chem. *78*, 6573–6582.

Crosse, A.M., Greenway, D.L., and England, R.R. (2000). Accumulation of ppGpp and ppGp in Staphylococcus aureus 8325-4 following nutrient starvation. Lett. Appl. Microbiol. *31*, 332–337.

D'Elia, M.A., Millar, K.E., Bhavsar, A.P., Tomljenovic, A.M., Hutter, B., Schaab, C., Moreno-Hagelsieb, G., and Brown, E.D. (2009). Probing teichoic acid genetics with bioactive molecules reveals new interactions among diverse processes in bacterial cell wall biogenesis. Chem. Biol. *16*, 548–556.

Debarbouille, M., Dramsi, S., Dussurget, O., Nahori, M.A., Vaganay, E., Jouvion, G., Cozzone, A., Msadek, T., and Duclos, B. (2009). Characterization of a serine/threonine kinase involved in virulence of Staphylococcus aureus. J. Bacteriol. *191*, 4070–4081.

Deutscher, J., Francke, C., and Postma, P.W. (2006). How phosphotransferase system-related protein phosphorylation regulates carbohydrate metabolism in bacteria. Microbiol. Mol. Biol. Rev. *70*, 939–1031.

Donat, S., Streker, K., Schirmeister, T., Rakette, S., Stehle, T., Liebeke, M., Lalk, M., and Ohlsen, K. (2009). Transcriptome and functional analysis of the eukaryotic-type serine/threonine kinase PknB in Staphylococcus aureus. J. Bacteriol. *191*, 4056–4069.

Ewald, J.C., Heux, S., and Zamboni, N. (2009). High-throughput quantitative metabolomics: workflow for cultivation, quenching, and analysis of yeast in a multiwell format. Anal. Chem. *81*, 3623–3629.

Feng, H.T., Wong, N., Wee, S., and Lee, M.M. (2008). Simultaneous determination of 19 intracellular nucleotides and nucleotide sugars in Chinese Hamster ovary cells by capillary electrophoresis. J. Chromatogr. B Analyt. Technol. Biomed. Life Sci. *870*, 131–134.

Fiehn, O., Kopka, J., Dormann, P., Altmann, T., Trethewey, R.N., and Willmitzer, L. (2000). Metabolite profiling for plant functional genomics. Nat. Biotechnol. *18*, 1157–1161.

Fiuza, M., Canova, M.J., Patin, D., Letek, M., Zanella-Cleon, I., Becchi, M., Mateos, L.M., Mengin-Lecreulx, D., Molle, V., and Gil, J.A. (2008). The MurC ligase essential for peptidoglycan biosynthesis is regulated by the serine/threonine protein kinase PknA in Corynebacterium glutamicum. J. Biol. Chem. *283*, 36553–36563.

Hanko, V.P., and Rohrer, J.S. (2000). Determination of carbohydrates, sugar alcohols, and glycols in cell cultures and fermentation broths using high-performance anion-exchange chromatography with pulsed amperometric detection. Anal. Biochem. *283*, 192–199.

Hecker, M., Reder, A., Fuchs, S., Pagels, M., and Engelmann, S. (2009). Physiological proteomics and stress/starvation responses in Bacillus subtilis and Staphylococcus aureus. Res. Microbiol. *160*, 245–258.

Heinemann, M., Kummel, A., Ruinatscha, R., and Panke, S. (2005). In silico genome-scale reconstruction and validation of the Staphylococcus aureus metabolic network. Biotechnol. Bioeng. *92*, 850–864.

Hutchison, K.W., and Hanson, R.S. (1974). Adenine nucleotide changes associated with the initiation of sporulation in Bacillus subtilis. J. Bacteriol. *119*, 70–75.

Katajamaa, M., Miettinen, J., and Oresic, M. (2006). MZmine: toolbox for processing and visualization of mass spectrometry based molecular profile data. Bioinformatics *22*, 634–636.

Kind, T., Scholz, M., and Fiehn, O. (2009). How large is the metabolome? A critical analysis of data exchange practices in chemistry. PLoS ONE *4*, e5440.. 10.1371/journal.pone.0005440.

Komatsuzawa, H., Fujiwara, T., Nishi, H., Yamada, S., Ohara, M., McCallum, N., Berger-Bachi, B., and Sugai, M. (2004). The gate controlling cell wall synthesis in Staphylococcus aureus. Mol. Microbiol. *53*, 1221–1231.

Kose, F., Budczies, J., Holschneider, M., and Fiehn, O. (2007). Robust detection and verification of linear relationships to generate metabolic networks using estimates of technical errors. BMC Bioinformatics *8*, 162.. 10.1186/1471-2105-8-162.

Lazzarino, G., Amorini, A.M., Fazzina, G., Vagnozzi, R., Signoretti, S., Donzelli, S., Di Stasio, E., Giardina, B., and Tavazzi, B. (2003). Single-sample preparation for simultaneous cellular redox and energy state determination. Anal. Biochem. *322*, 51–59.

Liebeke, M., Pother, D.C., van Duy, N., Albrecht, D., Becher, D., Hochgrafe, F., Lalk, M., Hecker, M., and Antelmann, H. (2008). Depletion of thiol-containing proteins in response to quinones in Bacillus subtilis. Mol. Microbiol. *69*, 1513–1529.

Liebeke, M., Brozel, V.S., Hecker, M., and Lalk, M. (2009). Chemical characterization of soil extract as growth media for the ecophysiological study of bacteria. Appl. Microbiol. Biotechnol. *83*, 161–173.

Lomas-Lopez, R., Paracuellos, P., Riberty, M., Cozzone, A.J., and Duclos, B. (2007). Several enzymes of the central metabolism are phosphorylated in Staphylococcus aureus. FEMS Microbiol. Lett. *272*, 35–42.

Lowy, F.D. (1998). Staphylococcus aureus infections. N. Engl. J. Med. *339*, 520–532.

Meyer, H., Liebeke, M., and Lalk, M. (2010). A protocol for the investigation of the intracellular Staphylococcus aureus metabolome. Anal. Biochem. *401*, 250–259.

Meyer, S., Noisommit-Rizzi, N., Reuss, M., and Neubauer, P. (1999). Optimized analysis of intracellular adenosine and guanosine phosphates in Escherichia coli. Anal. Biochem. *271*, 43–52.

Nordmann, P., Naas, T., Fortineau, N., and Poirel, L. (2007). Superbugs in the coming new decade; multidrug resistance and prospects for treatment of Staphylococcus aureus, Enterococcus spp. and Pseudomonas aeruginosa in 2010. Curr. Opin. Microbiol. *10*, 436–440.

Novakova, L., Saskova, L., Pallova, P., Janecek, J., Novotna, J., Ulrych, A., Echenique, J., Trombe, M.C., and Branny, P. (2005). Characterization of a eukaryotic type serine/threonine protein kinase and protein phosphatase of Streptococcus pneumoniae and identification of kinase substrates. FEBS J. *272*, 1243–1254.

Ohlsen, K., and Donat, S. (2009). The impact of serine/threonine phosphorylation in Staphylococcus aureus. Int. J. Med. Microbiol. *300*, 137–141.

Parikh, A., Verma, S.K., Khan, S., Prakash, B., and Nandicoori, V.K. (2009). PknB-mediated phosphorylation of a novel substrate, N-acetylglucosamine-1-phosphate uridyltransferase, modulates its acetyltransferase activity. J. Mol. Biol. *386*, 451–464.

Payne, D.J. (2008). Microbiology. Desperately seeking new antibiotics. Science *321*, 1644–1645.

Richardson, A.R., Libby, S.J., and Fang, F.C. (2008). A nitric oxide-inducible lactate dehydrogenase enables Staphylococcus aureus to resist innate immunity. Science *319*, 1672–1676.

Saeed, A.I., Sharov, V., White, J., Li, J., Liang, W., Bhagabati, N., Braisted, J., Klapa, M., Currier, T., Thiagarajan, M., et al. (2003). TM4: a free, open-source system for microarray data management and analysis. Biotechniques *34*, 374–378.

Schneider, T., Senn, M.M., Berger-Bachi, B., Tossi, A., Sahl, H.G., and Wiedemann, I. (2004). In vitro assembly of a complete, pentaglycine interpeptide bridge containing cell wall precursor (lipid II-Gly5) of Staphylococcus aureus. Mol. Microbiol. *53*, 675–685.

Sezonov, G., Joseleau-Petit, D., and D'Ari, R. (2007). Escherichia coli physiology in Luria-Bertani broth. J. Bacteriol. *189*, 8746–8749.

Sink, R., Kovac, A., Tomasic, T., Rupnik, V., Boniface, A., Bostock, J., Chopra, I., Blanot, D., Masic, L.P., Gobec, S., et al. (2008). Synthesis and biological evaluation of N-acylhydrazones as inhibitors of MurC and MurD ligases. ChemMedChem *3*, 1362–1370.

Somerville, G.A., and Proctor, R.A. (2009). At the crossroads of bacterial metabolism and virulence factor synthesis in Staphylococci. Microbiol. Mol. Biol. Rev. *73*, 233–248.

Sumner, L.W., Amberg, A., Barrett, D., Beale, M.H., Beger, R., Daykin, C.A., Fan, T.W.M., Fiehn, O., Goodacre, R., Griffin, J.L., et al. (2007). Proposed minimum reporting standards for chemical analysis. Metabolomics *3*, 211–221.

Tynecka, Z., Szczesniak, Z., Malm, A., and Los, R. (1999). Energy conservation in aerobically grown Staphylococcus aureus. Res. Microbiol. *150*, 555–566.

van der Werf, M.J., Overkamp, K.M., Muilwijk, B., Coulier, L., and Hankemeier, T. (2007). Microbial metabolomics: toward a platform with full metabolome coverage. Anal. Biochem. *370*, 17–25.

van der Werf, M.J., Overkamp, K.M., Muilwijk, B., Koek, M.M., van der Werff-van der Vat, B.J.C., Jellema, R.H., Coulier, L., and Hankemeier, T. (2008). Comprehensive analysis of the metabolome of Pseudomonas putida S12 grown on different carbon sources. Mol. Biosyst. *4*, 315–327.

Villas-Boas, S.G., Mas, S., Akesson, M., Smedsgaard, J., and Nielsen, J. (2005). Mass spectrometry in metabolome analysis. Mass Spectrom. Rev. *24*, 613–646.

Weidenmaier, C., and Peschel, A. (2008). Teichoic acids and related cell-wall glycopolymers in Gram-positive physiology and host interactions. Nat. Rev. Microbiol. *6*, 276–287.

Xia, G., and Peschel, A. (2008). Toward the pathway of S. aureus WTA biosynthesis. Chem. Biol. *15*, 95–96.

